52. B. Gomez-Lor, E. Guiterrez-Puebla, M. Iglesias, M. A. Monge, C. Ruiz-Valero, N. Snejko, *Inorg. Chem.* **2002**, *41*, 2429.
53. J. Perles, M. Iglesias, M.-A. Martín-Luengo, M. Á. Monge, C. Ruiz-Valero, N. Snjeko, *Chem. Mater.* **2005**, *17*, 5837.
54. U. Mueller, M. Stoesser, R. Ruppel, E. Baum, E. Bohres, M. Sigl, L. Lobree, O. M. Yaghi, M. Eddaoudi, WO 03/035717, assigned to BASF Aktiengesellschaft, 2003.
55. O. R. Evans, H. L. Ngo, W. Lin, *J. Am. Chem. Soc.* **2001**, *123*, 10395.
56. F. Molnar, G. A. Luinstra, M. Allmendinger, B. Rieger, *Chem. Eur. J.* **2003**, *9*, 1273.
57. H. S. Kim, J. J. Kim, S. D. Lee, M. S. Lah, D. Moon, H. G. Jang, *Chem. Eur. J.* **2003**, *9*, 678.
58. J. L. C. Rowsell, A. R. Millward, K. S. Park, O. M. Yaghi, *J. Am. Chem. Soc.* **2004**, *126*, 5666.
59. L. Pan, M. B. Sander, X. Huang, J. Li, M. Smith, E. Bittner, B. Bockrath, J. K. Johnson, *J. Am. Chem. Soc.* **2004**, *124*, 1308.
60. F. Millange, C. Serre, G. Férey, *Chem. Commun.* **2002**, 822.
61. E. Y. Lee, M. P. Suh, *Angew. Chem. Int. Ed.* **2004**, *43*, 2798.
62. X. Zhao, B. Xiao, A. J. Fletcher, K. M. Thomas, D. Bradshaw, M. J. Rosseinsky, *Science* **2004**, *306*, 1012.
63. B. Kesanli, Y. Cui, M. R. Smith, E. W. Bittner, B. C. Bockrath, W. Lin, *Angew. Chem.* **2005**, *117*, 74 and *Angew. Chem. Int. Ed.* **2005**, *44*, 72.
64. L.-G. Qiu, A.-J. Xie, L.-D. Zhang, *Adv. Mater.* **2005**, *17*, 689.
65. C.-D. Wu, A. Hu, L. Zhang, W. Lin, *J. Am. Chem. Soc.* **2005**, *127*, 8940.
66. T. Sawaki, T. Dewa, Y. Aoyama, *J. Am. Chem. Soc.* **1998**, *120*, 8539.
67. H. L. Ngo, A. Hu, W. Lin, *J. Mol. Catal. A: Chemical* **2004**, *215*, 177.
68. A. Hu, H. L. Ngo, W. Lin, *J. Am. Chem. Soc.* **2003**, *125*, 11490.
69. A. Hu, H. L. Ngo, W. Lin, *Angew. Chem. Int. Ed.* **2003**, *42*, 6000.
70. J. S. Seo, D. Whang, H. Lee, S. I. Jun, J. Oh, Y. J. Jeon, K. Kim, *Nature* **2000**, *404*, 982.
71. U. Mueller, G. Luinstra, O. M. Yaghi, O. Metelkina, M. Stoesser, WO 2004/037895, assigned to BASF Aktiengesellschaft/The Regents of the University of Michigan, 2004.
72. E. Guitérrez-Puebla, C. Cascales-Sedano, B. Gómez-Lor, M. M. Iglesias-Hernandez, M. A. Monge-Bravo, C. Ruiz-Valero, N. Snejko, ES 2,200,681, assigned to Consejo Superior de Investigaciones Cientificas Serrano, 2004.
73. B. Xing, M.-F. Choi, B. Xu, *Chem. Eur. J.* **2002**, *8*, 5028.
74. S. De Rosa, G. Giordano, T. Granato, A. Katovic, A. Siciliano, F. Tripicchio, *J. Agric. Food Chem.* **2005**, *53*, 8306.
75. B. Gómez-Lor, E. Guitérrez-Puebla, M. Iglesias, M. A. Monge, C. Ruiz-Valero, N. Snjeko, *Chem. Mater* **2005**, *17*, 2568.
76. M. Fujita, Y. J. Kwon, S. Washizu, K. Ogura, *J. Am. Chem. Soc.* **1994**, *116*, 1151.
77. O. Ohmori, M. Fujita, *Chem. Commun.* **2004**, 1586.
78. S. Takizawa, H. Somei, D. Jayaprakash, H. Sasai, *Angew. Chem. Int. Ed.* **2003**, *42*, 5711.
79. J. M. Tanski, P. T. Wolczanski, *Inorg. Chem.* **2001**, *40*, 2026.
80. L. Alaerts, E. Séguin, H. Poelman, F. Thibault-Starzyk, P. A. Jacobs, D. E. De Vos, *Chem. Eur. J.* **2006**, *12*, 7353.
81. T. Sato, W. Mori, C. N. Kato, T. Ohmura, T. Sato, K. Yokoyama, S. Takamizawa, S. Naito, *Chem. Lett.* **2003**, *32*, 854.
82. R. Tannenbaum, *Chem. Mater.* **1994**, *6*, 550.
83. R. Tannenbaum, *J. Molec. Catal. A: Chemical* **1996**, *107*, 207.
84. I. Feinstein-Jaffe, A. Efraty, *J. Molec. Catal.* **1987**, *40*, 1.

2.3.9 Oxo-Anion Modified Oxides

*Friederike C. Jentoft**

2.3.9.1 Introduction

2.3.9.1.1 Classification In the interaction of two or more catalyst components, two extremes can be found: the formation of a compound or a solid solution constitutes the most intimate and homogeneous type of interaction, while the formation of a non-wetting surface species on an inert support can be seen as the minimal type of interaction. For supported catalysts, the goal is usually the dispersion of the active species; the structural integrity of the support remains unchanged, although strong interactions may occur at the interface of the support and the dispersed phase (see Chapter 3.2.5). In this sense, anion-modified oxides such as sulfated or tungstated zirconia or sulfated titania could simply be understood as supported systems, specifically as mounted acids. In a typical preparation route, however, the second component (sulfate, tungstate) is added early in the preparation and is already present when the support or, better, ''matrix oxide'' crystallizes during the thermal treatment. As a consequence, the textural and structural properties (zirconia features a particularly vivid phase chemistry) of the matrix oxide are severely influenced by the additive. If further components such as promoters are added, the situation will become more complex. Although the product might be considered a surface-functionalized oxide, the systems are characterized by a strong interaction of the functionalizing agent and the matrix, leading to a mutual directing of their structures. The final product ideally contains only the matrix oxide as crystalline phase. This characteristic distinguishes these systems from coprecipitated catalysts such as Ni/Al_2O_3 and Cu/ZnO, which also feature precursors with intimate mixing of the components, but the final product obtained after a reduction step consists of separate phases, which are individually detectable by diffraction. Oxo-anion-modified oxides can thus be viewed as a separate class of catalysts.

2.3.9.1.2 Variety of Materials and Focus The lead system discussed in this chapter is sulfated zirconia but other varieties of this type of catalyst, that is, other anions and other oxides are also discussed. Sulfated zirconia was first described in a patent by Holm and Bailey in 1962 [1]. Profound interest in the system was raised years later through two articles by Hino and Arata, who reported

* Corresponding author.

sulfated zirconia to be active for *n*-butane isomerization at room temperature; that is, under conditions that thermodynamically favor the desired branched isomer [2, 3]. Commercialization of sulfated zirconia by UOP has been reported [4, 5], emphasizing the significance of this catalyst. Sulfated zirconia can be employed for a number of different reactions, most of which are acid-catalyzed processes; e.g. alkylation, condensation, etherification, acylation, esterification, nitration, and oligomerization [6].

Both catalyst components can be varied, i.e. (i) zirconia can be mixed with other oxides [7], or other matrix oxides or mixtures thereof can be employed and (ii) other oxo-anions can be used. For example, sulfated TiO_2, HfO_2, SnO_2 and Fe_2O_3 are each active for the skeletal isomerization of *n*-butane to isobutane at low temperatures [8]. Sulfated SiO_2 is active for the dehydration of ethanol [8]. ZrO_2 combined with tungstate is a catalyst for alkane isomerization [9, 10] and cracking [11], ZrO_2 with molybdate for conversion of hexane or benzoylation of toluene with benzoic anhydride [10] and ZrO_2 with borate for benzoylation of anisole with benzoyl chloride [12]. Materials obtained by treating ZrO_2 with SeO_4^{2-}, TeO_4^{2-} and CrO_4^{2-} are active for alkane dehydrogenation [8]. As a selection of combinations containing neither sulfate nor zirconia, tungstated SnO_2, TiO_2 and Fe_2O_3 may be named [10]; numerous other combinations can be imagined.

The activity of sulfated zirconia for butane isomerization can be further improved by orders of magnitude through the addition of cations of Fe and Mn [13, 14], or, e.g., Co or Ni [15]. Equally, tungstated zirconia can be promoted with, for example, Fe [16]. In general, sulfated or tungstated zirconia catalysts deactivate rapidly [17, 18], but by adding a noble metal to the catalyst, and hydrogen to the feed, the isomerization activity can be stabilized [16, 19, 20]. A complete catalyst thus consists of up to four types of components: the matrix oxide(s), the oxo-anion(s), promoters (optionally), and noble metal(s).

2.3.9.2 Target Properties

Three types of correlations have been made, namely between (i) performance and a measured or known physical quantity, (ii) performance and a preparation parameter or an observable that is characteristic of the preparation procedure, and (iii) physical quantities and a preparation parameter. Correlations of the first type allow for a targeted synthesis but still one must identify relationships between physical quantities and preparation parameters.

2.3.9.2.1 Structure–Activity Relationships

Unless they are noble-metal doped and operated in the presence of H_2, sulfated zirconia catalysts usually do not exhibit a stable performance. Thus, for any correlation it should be specified whether the maximum or steady-state activity has been evaluated.

The phase composition of zirconia has been identified as important. Zirconia occurs as three polymorphs, with the monoclinic phase being the room-temperature-stable modification. Above 1443 K, the tetragonal modification is preferred, whereas beyond 2643 K the cubic phase becomes stable [21]. The monoclinic phase of zirconia has been reported as inactive [22], or at least a factor of four to five less active than tetragonal zirconia [23]. Consistent with insignificant activity of the monoclinic phase, maximum *n*-butane conversion (or isomerization rate) was found to be proportional to the fraction of tetragonal phase [24, 25]. However, the presence of the tetragonal phase is only a necessary but not a sufficient requirement for good catalytic activity [26]; that is, not all tetragonal materials are automatically good catalysts. Sulfated zirconia that does not exhibit a distinct diffraction pattern has been claimed to be more [27] or less [28] active than conventional sulfated zirconia.

Catalytic activity is related to the surface area, for example in the case of butane isomerization [29, 30] or toluene cracking [31]. For the liquid-phase acylation of anisole with benzoyl chloride, the conversion is linearly related to the surface area, and increases monotonously with pore diameter in the range of 4.5 to 10.5 nm [32].

The sulfur content is also an essential parameter. For toluene benzylation, conversion increases linearly in the range of 0.01 to 0.023% S per m^2 g^{-1}, which should correspond to densities of two to four S atoms per nm^2 [33]. However, the conversion of methylcyclopentane passes through a maximum at an intermediate sulfate content [34]. The *n*-butane isomerization activity of Pt-doped sulfated zirconia increases with increasing sulfur content up to a level of ca. one S atom per nm^2, and then remains constant [35]. Other sources report distinct maxima in the isomerization rate of sulfated zirconia for sulfur contents of 170 μg m^{-2} (3 S atoms per nm^{-2}) [37], or 1–2 wt.% S [38], or 2.6 wt.% S [30]. There is evidence that a disulfate surface structure ($S_2O_7^{2-}$) is relevant for good performance in *n*-butane isomerization, and this condensation product is only formed at high sulfate surface density upon dehydration [38–42].

The highest butane isomerization rates per m^2 are observed at a Brønsted-to-Lewis site ratio of 1 after activation (as determined by pyridine adsorption) [36]. The Brønsted-to-Lewis sites ratio increases with increasing sulfate content. Unfortunately, the correctness of the number of Lewis sites as obtained by pyridine adsorption has been questioned, as this strong nucleophile may substitute for sulfate as a ligand of Zr ions and the Lewis acid sites will be overdetermined [43]. Correlations of the

References see page 275

reaction rate to the total number of acid sites as measured by ammonia adsorption are not always convincing; for example, a poor correlation was obtained for an acylation reaction [44], but good correlations were observed for 2-propanol dehydration and cumene dealkylation [45]. On the other hand, the *n*-butane isomerization rate was found to be proportional to the number of Brønsted acid sites as determined by pyridine adsorption [46].

Therefore, a preparative goal should be to maximize the fraction of tetragonal zirconia which, in the overwhelming proportion of reports, has been found more active in comparison to monoclinic or amorphous zirconia. A second goal is to maximize the surface area. Attempts have been made simply to support sulfated zirconia (or other oxo-anion modified oxides) on oxides with a higher surface area (such systems are not described here, but further information is available elsewhere [47–51]). The target with respect to the sulfate content is less clear. There appears to be an optimum, because Brønsted and Lewis sites are both necessary and the fraction of Brønsted sites increases with increasing sulfate content. On the other hand, a disulfate structure seems to be desirable, and such a condensed species forms preferably with increasing sulfate surface density. Furthermore, the described properties are not independent of each other due to the strong interaction between oxo-anion and matrix oxide.

2.3.9.2.2 **Effect of Sulfate and Other Oxo-Anions** The sulfate content influences the structural and textural properties of the final product. While pure zirconia, depending upon temperature, crystallizes into a mixture of monoclinic and tetragonal zirconia, the tetragonal phase becomes increasingly predominant as the sulfate content is raised [52]. No general statement can be made as to the amount of sulfate necessary to obtain solely tetragonal zirconia, because the phase composition depends also strongly on the calcination conditions (*vide infra*).

The surface area was found to be a linear function of the sulfate content up to about 5 wt.% SO_4^{2-}, with a slope of 30 $m^2\ g^{-1}$ per wt.% SO_4^{2-} for ZrO_2, TiO_2 and SnO_2, and a slope of 8 $m^2\ g^{-1}$ per wt.% SO_4^{2-} for Al_2O_3 and Fe_2O_3 [31]. The linear correlation can be interpreted as the stabilization of a certain area per sulfate group, namely 0.5 nm^2 for oxides with the stoichiometry MO_2, or 0.14 nm^2 for the M_2O_3 type. Other studies confirm the surface area increase up to a content of 4–6 wt.% SO_4^{2-}; at higher loadings, the data are not consistent [37, 53]. Anions such as sulfate, tungstate, and molybdate have the same effect, as can be seen in Fig. 1 [52, 54]. The relative weights of WO_3, MoO_3, and SO_4^{2-} explain the offset of the curves with respect to content. The attainable surface area, however, is considerably higher for WO_3/ZrO_2 and MoO_3/ZrO_2. For sulfated zirconia, the surface area decreases at higher calcination temperatures, and the maximum shifts to lower sulfate contents, as Fig. 2 demonstrates.

At very high sulfate contents, the surface area decreases (see Fig. 1), and the size of the tetragonal crystallites increases (based on analysis of the line width with the Scherrer formula) [55, 56]. No systematic trend in the porosity with the sulfur content could be found [52]. A maximum in the number of Brønsted sites (as measured by pyridine adsorption) is found at around four S atoms per nm^2 [57].

A high sulfate content is desirable because the active condensed sulfate structure seems to form only when

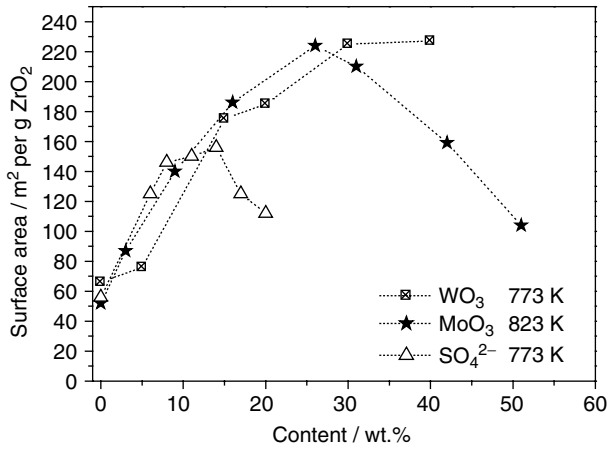

Fig. 1 Surface area as a function of modifier content, with modifier type as a parameter. (After Ref. [54].)

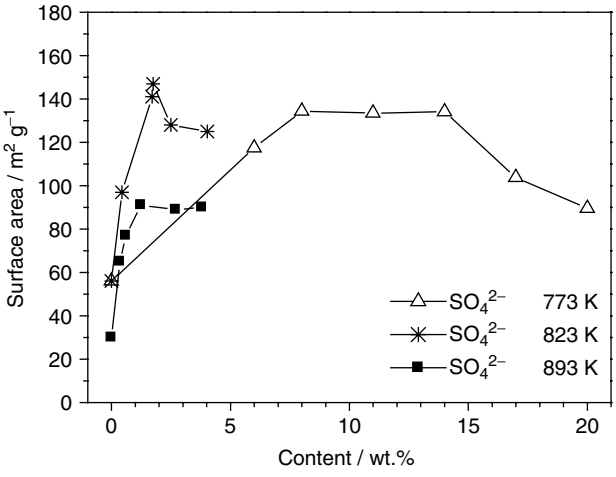

Fig. 2 Surface area as a function of sulfate content, with calcination temperature as a parameter. (After Refs. [35, 52, 54].)

a sufficient sulfate density is reached on the surface; furthermore, the surface area increases with sulfate content. However, very high sulfate contents have negative effects. The sulfate content may be controlled through the sulfation procedure only if it is ensured that there will be no sulfur loss during calcination.

2.3.9.3 Preparation Routes

The typical preparation route of sulfated zirconia and related materials follows the classical sequence according to IUPAC [58]: formation of a primary solid with all components, thermal treatment, and activation. The principles of preparing a precursor for the matrix oxide by precipitation or sol–gel synthesis are presented in Chapters 2.3.3 and 2.3.4. of this handbook. The procedures for dispersing noble metals are discussed in Chapter 2.4.2. However, oxo-anions, promoters, and noble metals can be associated at different stages of the preparation (see Fig. 3). The main theme of this chapter is to develop an understanding for the interaction of oxide precursor, oxo-anion, and promoters during formation of the primary solid or during thermal treatment and for the ensuing solid state chemistry, and from this knowledge to recommend suitable compositions and preparation procedures.

2.3.9.4 Formation of Primary Solid

To produce a suitable precursor for a high-surface-area zirconia, the starting point is usually a zirconium species dissolved in liquid phase. The zirconium reagent may be either an inorganic salt or an organyl.

Zirconium salt solutions have a number of industrial uses [59, 60] and their chemistry has been studied extensively [61–73]. In general, zirconium(IV) cations have a strong tendency to hydrolyze in aqueous medium; that is, the solutions are not stable and typically turn cloudy, which makes it difficult to exert control. Attempts have been made to identify the complexes that are formed in the hydrolysis reaction, as well as the species formed in subsequent reactions. Research has focused on solutions containing anions such as chloride, nitrate, and perchlorate, which are neither strongly complexing nor bridging. A discrete tetrameric complex, $[Zr_4(OH)_8(H_2O)_{16}]^{8+}$ is present; it can be neutralized through attachment of eight chloride ions [62, 63]. The tetrameric complex has been identified in zirconium oxychloride solutions [64, 68, 71], in zirconium perchlorate solutions [66], and in zirconium nitrate solutions [65]. Upon increase of temperature or *pH*, the tetramer will oligomerize presumably in a first step to an octamer [64, 71] of the constitution $[Zr_8(OH)_{20}(H_2O)_{24}Cl_{12}]$ [68], and then to higher oligomers, which will finally aggregate and precipitate. At 373 K, 3 to 7 nm primary particles were observed [67]; secondary particles (aggregates of primary particles) reach 175 to 250 nm [70, 72]. The particle growth rate can be decreased through addition of HCl [71]. Hence, the precipitation chemistry can be determined by concentration, *pH*, and temperature.

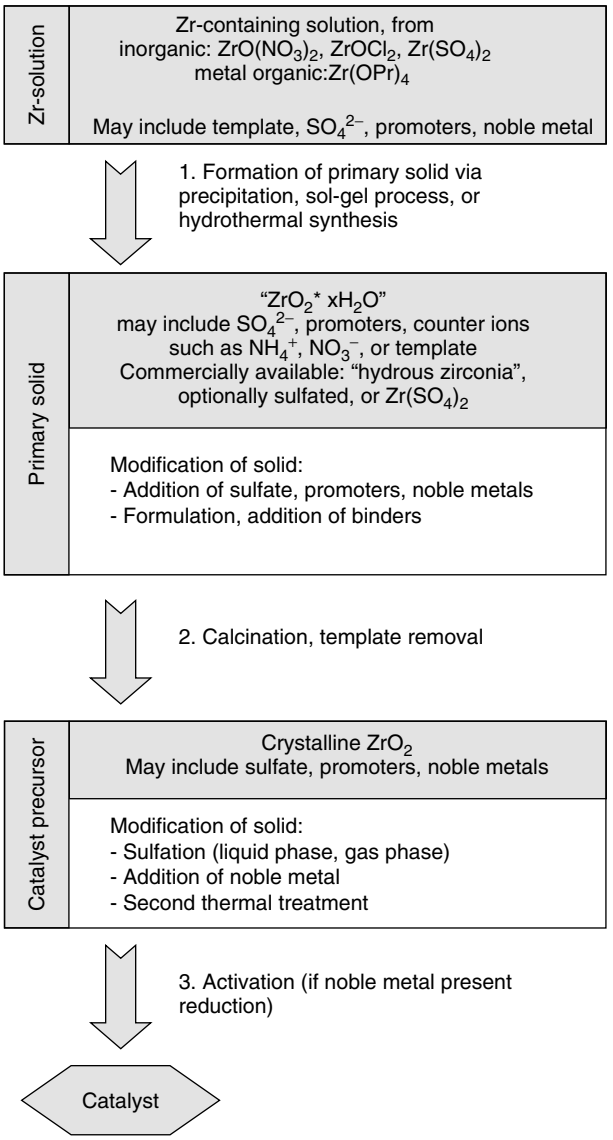

Fig. 3 General preparation scheme for sulfated zirconia as an example for an oxo-anion modified oxide.

The chemistry of zirconium sulfate solutions is different because sulfate not only strongly complexes with zirconium [74, 75] but also potentially acts as bridging ligand and promotes polymerization [75, 76]. While cationic or neutral complexes prevail in chloride, nitrate, and perchlorate solutions, anionic [77, 78] mixed

References see page 275

hydroxosulfato complexes [76], also of polynuclear type, are formed in sulfate solutions. Polynuclear complexes can form through different bridging mechanisms; that is, hydroxo bridges (formed in an ''olation'' reaction), oxo bridges (''oxolation''), and sulfato bridges. Sulfate-bridged complexes of the constitution $[Zr_n(OH)_{n+1}(SO_4)_{2n}]^{(n+1)-}$ have been proposed [76], or complexes of the type $[Zr(OH)_2(SO_4)_x(OH_2)_y]_n^{-n(2x-2)}$, which include water as a ligand [80]. Hence, it is not hydrous zirconia that is precipitated from these solutions, but sulfates; and the large number of possible sulfates [61, 81, 82], especially basic sulfates [61, 83–85], suggests that numerous complexes of different constitution may exist in solution. Consistently, no particular species have been reported as being stable over a range of conditions in zirconium sulfate solutions. The time frame for changes in these solutions [83] indicates that equilibration is slow: precipitation in 0.5 M $Zr(SO_4)_2$ solutions was observed only after 2 weeks [86], and precipitation in 0.2 mM $Zr(SO_4)_2$ could be delayed by 10 h, 2 days, or 4 days by dissolving the salt in 1, 2, or 4 mM HNO_3, respectively [77]. Heating promotes hydrolysis [87]. The kinetics of formation of larger particles in zirconium sulfate solutions have been investigated, and growth was accelerated at higher temperature, higher zirconium concentration and lower acid concentration [88]. From the available data it becomes clear that not only concentration, temperature and *pH*, but also aging, will play a role in the formation of the primary solid.

The chemistry in zirconium aqueous solutions depends strongly on the complexation with the available anions. Zr complexes may be either cationic or anionic, which also determines the choice of surfactant in a templated synthesis. In general, for each metal cation and each oxo-anion, their joint solution chemistry must be considered, and adding the oxo-anion during the formation of the primary solid may affect the properties of the matrix oxide significantly.

2.3.9.4.1 **Formation of Pure Hydrous Zirconia** Starting compounds used for the formation of hydrous zirconia are $ZrOCl_2$ [89], $ZrO(NO_3)_2$ [36], and zirconium alkoxides [28, 90]. Precipitating agents are aqueous ammonia [89] and solutions of either KOH or NaOH [91, 92]. The precipitates are of a gelatinous nature [89], and a crystalline zirconium hydroxide with a defined stoichiometry does not exist [93]. Hydrolysis of Zr alkoxides, which are soluble in for example ethanol, 1-propanol, 2-propanol or cyclohexane [44], can be initiated by water [94, 95], acids [90], or bases [33]. For other oxides, e.g. $TiCl_4$ or $SnCl_4$ are used as starting compounds.

The precipitation can be conducted either by adding the zirconium solution to the base, or by adding the base to the zirconium solution. A more dramatic effect than the method of addition has the subsequent ageing or digesting of the precipitate [89]. Figure 4 shows how the surface area and the fraction of tetragonal phase increase with increasing digestion temperature. Moreover, the surface area correlates with the fraction of tetragonal phase. The surface area increases with digestion time, for example from 48 $m^2\,g^{-1}$ without digestion to 248 $m^2\,g^{-1}$ after a 96-h digestion at 373 K and calcination at 773 K [89]. In addition, the pore size distribution becomes narrower [28]. Digestion at *pH* 14 (KOH or NaOH) produces materials with surface areas stable up to 773 K, while undigested materials or those digested at *pH* 11–9.4 (NH_4OH) lose surface area upon thermal treatment [91]. The acid site distribution is also altered; ammonia desorbs at higher temperatures from previously digested calcined zirconia, but the adsorbed amount per m^2 is unaffected [92].

Hydrous zirconia can also be prepared via hydrolysis of zirconium alkoxides. Variations of the water/alkoxide ratio between 2 and 32 were found to have only a minor influence on the surface area of calcined zirconia (773 K) in comparison to the digestion time [95]. The zirconia surface area was reported to increase until about 200 h of digestion time at *pH* 9, reaching values larger than 300 $m^2\,g^{-1}$. Digestion at *pH* 1 or 3 produces surface areas smaller than 100 $m^2\,g^{-1}$; in general the fraction of the monoclinic phase in the calcined material (773 K) increases with decreasing *pH* of the suspension [28, 95]. Zirconia gels can also be produced in supercritical CO_2 by hydrolyzing zirconium alkoxides with acetic acid [90].

2.3.9.4.2 **Formation of Sulfate-Containing Hydrous Zirconia** Sulfate can already be added during the formation

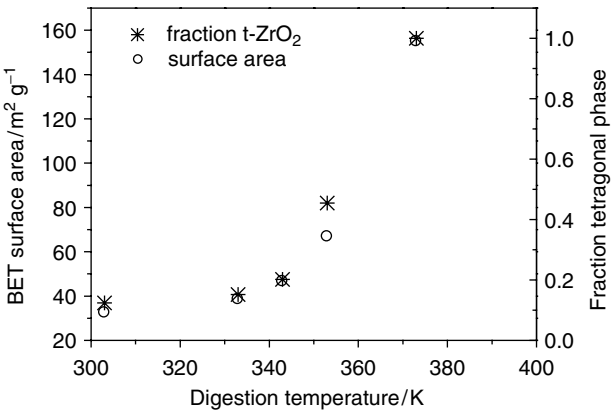

Fig. 4 Surface area and fraction of tetragonal phase as a function of digestion temperature. Basic precipitation, calcination at 873 K. (After Ref. [89].)

of the primary solid. In a synthesis via gel formation from alkoxides, sulfate can be introduced during the gelling step [53, 96, 97] or during peptization [98]. Tungstate can equally be co-gelled [99]. Reverse microemulsions can also be used as a synthesis medium for sulfated zirconia nanoparticles [100].

A large amount of sulfate can be incorporated into the primary solid due to the ability of sulfate to act as a bridging ligand between zirconium cations. The amount of sulfate can exceed 50 wt.% after application of sulfuric acid for peptization following a sol–gel synthesis; this will lead to sulfate contents of approximately 20 wt.% after calcination at 823 K [98]. For calcination temperatures below 873 K, samples co-gelled with sulfate exhibit higher surface areas than those sulfated with ammonium sulfate at a later stage [96]. The surface and bulk sulfate concentrations increase with increasing H_2O/Zr ratio [101]. The drying method has also been investigated, with a xerogel (regular drying) being more active in *n*-butane isomerization than an aerogel (supercritical drying) [102].

2.3.9.4.3 **Template-Directed Formation of Primary Solid** Supports such as silica can be synthesized in the form of mesoporous molecular sieves [103] (see also Chapter 2.3.6). These materials are characterized by a very high surface area, which would be desirable also for zirconia, and can be achieved via a template-assisted hydrothermal synthesis. Surfactant molecules assemble to micelles, which direct the growth of the oxide matrix from an organometallic precursor. The surfactant is later removed in a calcination step. The difficulty with zirconium is that, in the strongly acidic solutions required to restrict hydrolysis, it is present in the form of cationic complexes (see Section 2.3.9.4); the typically used surfactants are protonated under these conditions and hence assembly cannot take place [104]. One solution to this problem is the addition of sulfate to generate anionic zirconium species, but full condensation is apparently prevented and the framework may be partially destroyed when the sulfate is removed by calcination. Using hexadecyltrimethyl ammonium bromide as surfactant, it was possible to obtain an MCM-41-like structure, which collapsed during calcination [105]. Treatment of the as-synthesized composite with phosphoric acid stabilizes the structure throughout calcination, with S and P contents of 1 and 10 wt.%, respectively, in the final product. By using zirconium propoxide and ammonium sulfate instead of zirconium sulfate, an ordered pore system with S contents of up to 8.5 wt.% could be obtained [80]. Further procedures either with [106–108] or without [109] sulfate in the surfactant-containing synthesis mixtures have been published. The structural homogeneity and the catalytic properties of these materials vary. Inactivity in *n*-hexane isomerization was found combined with high activity for benzene alkylation with propene [106]. A lower activity in *n*-butane isomerization than for conventional tetragonal zirconia was observed for mesostructured zirconia [108], but a higher activity has also been reported [109].

2.3.9.4.4 **Commercially Available Precursors** Hydrous and sulfated hydrous zirconia materials are available, e.g., from MEL Chemicals or Sigma-Aldrich [110], and are frequently employed in both, academia and industry to produce sulfated zirconia catalysts [15, 111–113]. Zirconium compounds contain Hf as an impurity, e.g. hydrous zirconia contains typically about 1 wt.% Hf [112]. Zirconium sulfate, titanium sulfate and tin sulfate can also be used as precursors for the corresponding sulfated metal oxides [31, 114, 115].

2.3.9.5 **Anion-Modification of Primary Solid**

2.3.9.5.1 **Addition of Oxo-Anions to Primary Solid in Liquid Medium** Different sulfating agents are used for sulfation in aqueous solution: H_2SO_4, $(NH_4)_2SO_4$, HSO_3Cl [116], $(NH_4)_2S_2O_8$ [117, 118], and $Zr(SO_4)_2$ [119]. The procedures used are incipient wetness impregnation [35], soaking in excess impregnating solution and filtering (sometimes referred to as percolation) [52, 120], and soaking in excess impregnation solution followed by solvent evaporation [121]. Typical precursors for other oxo-anions are ammonium metatungstate $(NH_4)_6H_2W_{12}O_{40} \cdot x\,H_2O$ [8] or ammonium metamolybdate [122].

The surface sulfur content (calculated from total content and surface area with the assumption that all sulfate is on the surface) in the calcined and reduced catalysts increases linearly with the concentration of the H_2SO_4 used in an incipient wetness procedure [35]. When an excess of acid is applied and the solid is filtered, the total sulfate content in the calcined product increases first steeply (<0.5 M), and then linearly with H_2SO_4 concentration [52, 123]. A similar course is found for the sulfate surface density [118]. The surface sulfate content of the calcined materials (as measured by photoelectron spectroscopy) increases initially more steeply with increasing H_2SO_4 molarity than the total sulfate content [52]. The sulfate content increases with the amount of sulfuric acid used for the impregnation [34]. More sulfate can be deposited (solvent evaporation) than adsorbed (filtration) [124].

As a natural consequence of the described dependence of surface area on sulfate content, and the possible ways to modify the sulfate content by way of the impregnation

References see page 275

step, the surface area correlates with the amount of sulfate applied. These correlations all show maxima in the surface area, either at an intermediate H_2SO_4 amount [34], or at intermediate concentrations e.g., at 0.5 M H_2SO_4 [120] or 0.2–0.25 M H_2SO_4 [123]. A maximum surface area at 0.25 M H_2SO_4 coincides with the maximum in butane conversion [94]. The pore diameter decreases with the addition of sulfate, and remains constant at about 8 nm for H_2SO_4 concentrations larger than 0.05 M [120]. Not only the sulfate concentration but also the *pH* plays a role: the maximum surface area is attained when hydrous zirconia is soaked in a sulfate-containing solution of *pH* 6–9, and these samples also produce the maximum isobutane yield under steady-state conditions [125]. The precursors, which result in different *pH*, unless it is adjusted, are also important; for example, catalysts obtained via H_2SO_4 impregnation give a higher butane conversion than those from $(NH_4)_2S_2O_8$ impregnation [118]. Some authors prefer H_2SO_4 as sulfating agent [10], and others $(NH_4)_2SO_4$ [6].

2.3.9.5.2 **Sulfation of Primary Solid via Gas Phase** Treatment of hydrous zirconia with SO_2 enhances the activity for *n*-butane isomerization as much as impregnation with sulfuric acid, whereas treatment with H_2S or SO_3 does not produce active materials [2]. Silica gel can be treated with SO_2Cl_2, which reacts with the surface OH groups, in order to generate sulfate attached to silica [8].

2.3.9.5.3 **Introduction of Oxo-Anions Using Solid Precursors** Calcination of a kneaded mixture of hydrous zirconia and ammonium sulfate at 773 K produces a material that is active for butene double bond isomerization and benzoylation of anisole [126]. Kneading hydrous zirconia with H_2WO_4, followed by calcination, yields a catalyst for pentane conversion [8].

2.3.9.6 Addition of Promoters (Optional)

2.3.9.6.1 **Promoters** Of the main group elements, Al [117, 127–133] and Ga [24, 134] act as promoters of sulfated zirconia isomerization catalysts. First row transition metals such as Ti [127], V [127], Cr [127, 135], Mn [10, 15, 136–138], Fe [10, 15, 127, 135–137, 139–142], Co [15, 127, 135], and Ni [15, 127, 132, 135, 139, 143, 144] have attracted considerable attention. Nb is a promoter for alkane isomerization [145]. Silver and copper in the form Ag^0 and Cu^0 promote the activity of sulfated zirconia for *n*-pentane isomerization [146]. Ag and Cu are also suitable as additives to tungstated zirconia [147]. Ce and other lanthanides are also promoters of sulfated zirconia [112, 145].

Combinations of promoters have also been tested. In particular, the combination of Fe and Mn was studied in detail for isomerization [14, 127, 136, 137, 139, 148–171], and also for cracking [172–174] and alkylation reactions [175], since a synergistic effect between the two promoters was reported. Other successful combinations include Cr–Fe and V–Fe [127].

2.3.9.6.2 **Structure–Activity Relationships** A number of relationships concerning performance and promoters have been reported. The efficacy of the first row transition metal promoters follows a trend in the Periodic Table, that is, under the selected conditions, the maximum activity decreases in the order Mn > Fe ≫ Co > Ni ≫ Zn [15]. The conversion of *n*-pentane increases with decreasing ionic radius of the promoter cation in eightfold coordination; this relationship applies to yttrium and lanthanides [112].

The promoter content can be optimized [117, 144], and, e.g., when combining Group V, VI, and VII elements, the sum of all promoters is ideally between 0.1 and 4.5 wt.% metal [13]. The relationship between the conversion to isobutane and promoter content depends on the promoter type [139]. The steady-state *n*-butane isomerization rate was found to increase with an increasing ratio of the lattice constant c/a of the tetragonal phase for a family of Fe- or Mn-promoted catalysts [176].

2.3.9.6.3 **Effect of Promoters** Promoters such as Mn or Fe stabilize the desired tetragonal phase of zirconia and, at high content, the cubic phase [113]. Stabilization of the high-temperature phases is a result of the incorporation of the promoter cations into the zirconia lattice [113]. This phenomenon is well known for ions of e.g. Y, Ca, or Mg; because of its wide application as a ceramic material yttria-stabilized zirconia has been studied extensively [177]. Many cations can be dissolved in the zirconia lattice [178–181]. The lattice parameters of the stabilized tetragonal or cubic phase vary, depending on promoter type and content. The lattice may either contract or expand, with a linear relationship between certain lattice parameters and the molar fraction of promoter, corresponding to Vegard's law [181]. For example, Mn or Fe cause a contraction [113]. In light of the formation of solid solutions it can be understood why pentane conversion and ionic radius of the promoter are correlated [112]. The valence of the promoter ions differs from that of zirconium, and charges must be compensated in the lattice, for example by creating oxygen vacancies to balance the incorporation of ions with a valence less than +IV. Hence, the promoters alter the geometric and electronic structure of the zirconia matrix.

Promotion sometimes results in a slight increase in surface area [24, 134], but not on all occasions [144]. The differences in surface area seem to be more pronounced when the calcination produces an unpromoted sulfated zirconia with significant amounts of monoclinic phase, while the promoters stabilize the tetragonal phase with its typically higher surface area (see Fig. 4). A 0–67% higher sulfate content is observed in promoted compared to unpromoted sulfated zirconia samples [24, 127, 134]. The promoters affect the reducibility of the oxo-anions on zirconia. In the presence of Mn, Fe, or Ga, the reduction temperature of sulfate is decreased [134, 182, 183] and, in the presence of Ga, tungstate is more easily reducible [184].

While the choice of promoter type and content is straightforward, it is unclear whether the synthesis should target the dissolution of the promoter ions in the zirconia lattice or the formation of surface species. Evidence exists for both scenarios, that is either incorporated or surface promoter species may be catalytically relevant, as discussed in Ref. [113].

2.3.9.6.4 **Addition of Promoters** Promoters can be introduced at the solution stage before formation of the primary solid, they can be impregnated onto the primary solid, or they can be added to the crystalline oxide, always followed by calcination. It would seem that the first method should produce preferably incorporated species whereas the last method should produce preferably surface species. The literature though is not in agreement as to which method produces predominantly which species [113]. Figure 5 shows a more pronounced effect of the promoters on the lattice constant for preparation via coprecipitation in comparison to incipient wetness impregnation, suggesting that, indeed, incorporation is furthered when zirconium and promoter ion species are well interspersed in the primary solid.

Coprecipitation from a mixed solution of zirconium and promoter ions has been applied to introduce, for example, Al, Ga, Ti, Cr, Mn, Fe, Co, or Ni [24, 117, 127, 134]; the sulfate can be added later [127]. If the promoters are introduced by impregnating a solid and the oxo-anion is already present, then the solubility of the oxo-anion in the impregnation solution must be considered. Even after calcination, the sulfate in sulfated zirconia is water-soluble and will be partially removed in aqueous medium [113, 185]. One frequently applied method is that of incipient wetness [14, 15], in which the solubility problem is suppressed. The order of adding sulfate and promoters to the primary solid via incipient wetness impregnation does not result in significant differences in *n*-butane isomerization activity [186]. If Al- or Ga-promoted sulfated zirconia are prepared by first introducing the promoters and then the sulfate, coprecipitation yields superior catalysts in comparison to wet impregnation [24].

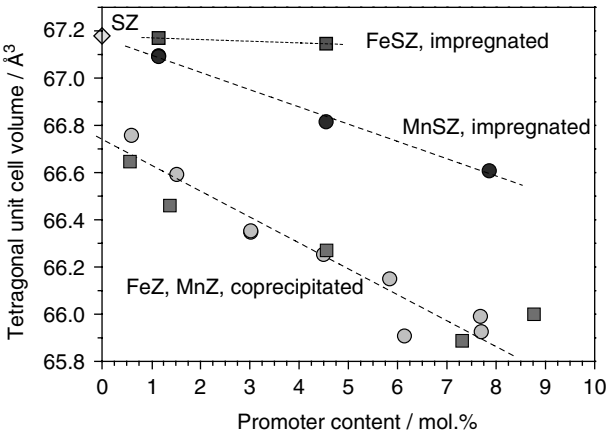

Fig. 5 Tetragonal unit cell volume as a function of promoter content with promoter type and promoter addition method as parameters. Circles, Mn promotion; squares, Fe promotion.

Calcination of physical mixtures of sulfated zirconia with $FeSO_4$, sulfated Fe_2O_3 or Fe_2O_3 at 723–873 K also results in catalysts with promoted activity in *n*-butane isomerization [187].

2.3.9.7 Calcination

2.3.9.7.1 **Events Occurring During Calcination** During calcination, a largely disordered hydroxide-type precursor is converted into a crystalline metal oxide. The chemical reactions that occur are dehydration and condensation reactions such as dehydroxylation, which leads to the formation of oxo-bridges (oxolation) between the metal cations [188]. Further components that are able to cleave out volatile compounds may be decomposed; for example, NH_3 may be released from ammonium, NO_x from nitrates, and SO_2 and O_2 from sulfate. Also from other oxo-anions volatile species may be produced, e.g. MoO_3. Redox processes can occur through reaction with the oxygen of the calcination atmosphere, or through re-reaction with volatilized species, affecting the valences of the catalyst components. Surfactant molecules would be combusted. Structure and morphology change considerably during calcination. The oxide crystallizes and particles coalesce, leading to a loss in surface area and a change in porosity.

Thermogravimetric (TG) and differential thermal analysis (DTA) data for an ammonium sulfate-treated hydrous zirconia are presented in Fig. 6 (for further data relating to zirconia-based materials, see Refs. [91, 136,

References see page 275

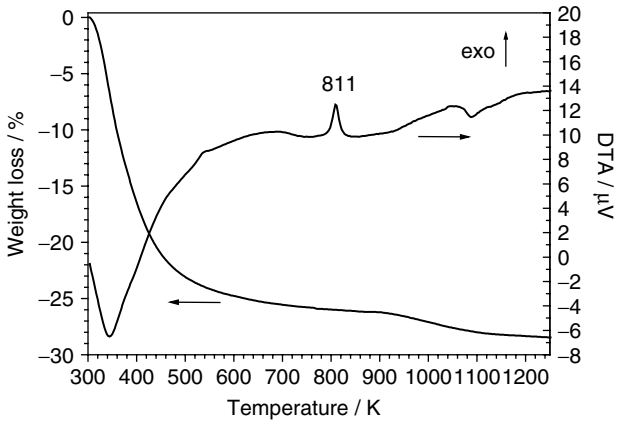

Fig. 6 Thermogravimetry and differential thermal analysis data for sulfated hydrous zirconia (MEL XZO 682). Heating rate 7 K min^{-1}.

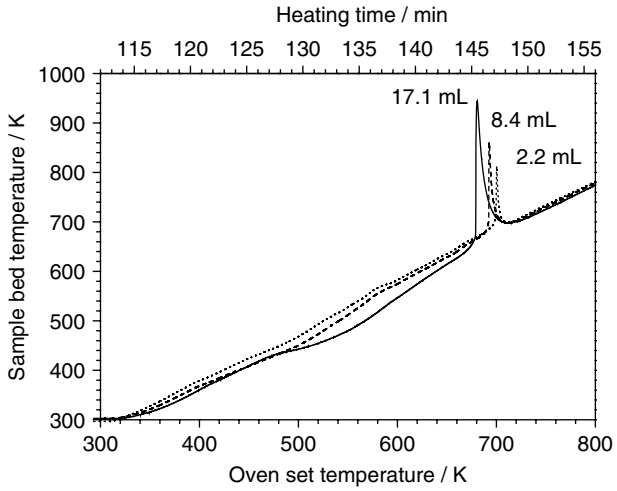

Fig. 7 Actual sample temperature of hydrous zirconia (center of bed) as a function of oven set temperature with precursor volume as a parameter. Heating rate 3 K min^{-1}; synthetic air flow 200 mL min^{-1}. Samples were placed in quartz boats of different volume [204].

189–191]). The TG curve is characterized by a large weight loss of more than 25% that extends to 873 K, and a second, smaller weight loss that sets in at about 900 K. The first loss is connected with the evaporation of water and the decomposition of ammonium, and the second loss to the decomposition of sulfate. The DTA curve shows the water loss and sulfate decomposition to be endothermic, and additionally shows an exothermic peak at about 800 K. The origin of this "glow exotherm" has been debated, whereby crystallization [192, 193], the loss of internal surface hydroxyl groups [194], and the coalescence of small particles to larger ones [195, 196] have been proposed as heat-generating processes.

The enthalpies derived from thermal analysis for, presumably, the crystallization of tetragonal or monoclinic zirconia show a wide spread, ranging from −4.3 to −58.6 kJ mol^{-1} [91, 191–193, 197–201]. The energetic difference between the two phases is small; the monoclinic is about 5 kJ mol^{-1} more stable [199, 202]. These discrepancies in enthalpy can be ascribed to variations in the initial and final states. The properties of "hydrous zirconia" depend strongly on the procedure of preparation, and this state is usually not closely investigated. The final state is also insufficiently characterized, in that only the detected phases are considered but not amorphous fractions or properties such as crystallite sizes and surface areas.

From the thermal analysis data it is obvious that, during calcination, considerable mass and heat transfer occurs which, particularly when working on a preparative scale, may be limited. The chemistry will be influenced by the mass transfer conditions, e.g. the condensation chemistry will be affected by the water vapor partial pressure in the pores and the surrounding gas phase. Surface diffusion and hence zirconia crystallite growth is reported to be accelerated by water vapor [203]. Any volatile species can potentially be re-deposited on the material's surface.

2.3.9.7.2 **Effect of Bed Volume and Packing** The actual sample temperature of hydrous zirconia during the heat-up phase of the calcination program is presented in Fig. 7. Significant deviations from the planned ramp are apparent, which differ depending on the sample volume employed [204, 205]. The sample temperature lags behind the oven set temperature, and more so with increasing sample volume, because of the endothermic evaporation of water. Retention of water vapor in a tightly packed bed will delay condensation reactions, which should lead to higher surface areas. At oven temperatures of 675 to 700 K, the bed temperature exhibits a brief, but significant, overshoot. For a 17.1-mL volume, the overshoot amounts to 260 K, with an increase of 45 K s^{-1}. The curves indicate explosion kinetics; heat cannot be dissipated as rapidly as it is produced. The onset shifts to lower temperature with increasing volume, probably due to a restricted heat transfer with the small surface-to-volume ratio and more complete enclosure of the bed in the larger quartz boats.

This violent reaction is designated in the literature as the "glow phenomenon", in reference to the emission of visible light, and was first reported by Berzelius in 1812 [206, 207]. For zirconia, it was mentioned already in 1818 [208] but was more thoroughly investigated only decades later [209, 210]. The phenomenon is also observed during the formation of chromium oxide, iron oxide and titania, and is thus of general relevance; however, it does not occur during alumina formation [195, 210]. Additives of any type shift the glow event to a higher temperature [189, 190, 196, 197, 204, 205] and

subdue or even suppress it [193, 195]; for sulfate, the exotherm temperature shifts linearly with content [190]. Estimation of the expected temperature overshoot from enthalpy changes due to crystallization or surface area loss, under the assumption of quasi-adiabatic conditions, shows that either process can account for the phenomenon [205].

The actual temperature curves during calcination for a sulfated hydrous zirconia material promoted with 0.5 wt.% Mn are shown in Fig. 8. The addition of sulfate and Mn shifts the onset of the overheating to about 100 K higher temperature. The nitrogen adsorption and desorption isotherms for the obtained materials are shown in Fig. 9. The hysteresis loop becomes more pronounced with increasing bed volume. The surface area increases slightly, from 92 to 96 to 106 $m^2\ g^{-1}$, consistent with the idea of inhibition of oxolation and coalescence by water retained in a larger bed. In Fig. 10, the catalytic activity data are presented for the same set of samples. The rates increase significantly with the volume used for the calcination, excluding surface area as the sole explanation for the differences.

These data show that variations in bed size and packing during calcination can produce different materials from a single precursor batch [204, 205]. Although the nominal conditions (heating ramp, holding temperature and time, atmosphere) are identical in these calcinations, the samples experience quite different actual conditions. During the initial phase, the water vapor partial pressure will affect the condensation chemistry. Crystallization starts before overheating is observed. Surface area and

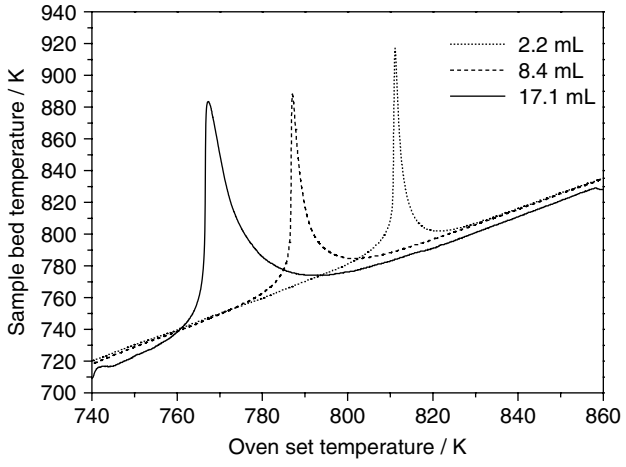

Fig. 8 Actual sample temperature of hydrous zirconia promoted with 0.5 wt.% Mn (center of bed) as a function of oven set temperature with precursor volume as a parameter. Heating rate 3 K min^{-1}; synthetic air flow 200 mL min^{-1}; holding time 3 h at 923 K. Samples were placed in quartz boats of different volume [204].

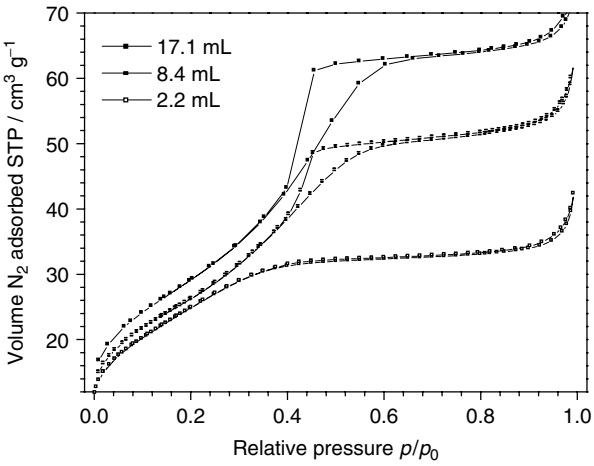

Fig. 9 Adsorption and desorption branches of nitrogen adsorption isotherms at 77 K. Sulfated zirconia promoted with 0.5 wt.% Mn.

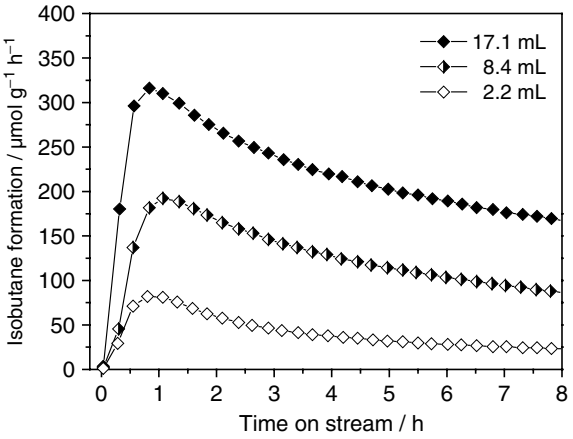

Fig. 10 Isobutane formation rate versus time on stream for sulfated zirconia promoted with 0.5 wt.% Mn. Activation: 0.5 h at 723 K in N_2. Reaction conditions: 500 mg catalyst, 1 kPa *n*-butane in N_2 at atmospheric pressure, 338 K, 80 mL min^{-1} total flow.

diffractogram of a sample that was cooled directly after the glow phenomenon largely correspond to those of samples that underwent the complete heating program, which indicates that structure and morphology are developed during overheating [205]. During the temperature overshoot, the desired maximum temperature may be exceeded, which allows for a chemistry that is not possible within the planned program. Enhanced ion mobility within the forming solid, as well as volatilization and reanchoring with a restructuring of surface species, can also be envisioned. Because of the fairly rapid cooling down following the overshoot, non-equilibrium states might be

References see page 275

quenched. The subsequent holding time at high temperature does not equalize differences evoked during the heat-up phase. Consistently, attempts have been made to relate high *n*-pentane isomerization activity to a sharp and high exothermal peak [191]. In part, the reported lack of reproducibility [211] of these catalysts may originate from underestimating the importance of the details of the calcination procedure. Samples calcined in different set-ups are not comparable on an absolute scale, and the data discussed below illustrate such trends.

2.3.9.7.3 **Effect of Calcination Temperature on Physical Properties** The calcination temperature has a major influence on phase composition, surface area, and sulfate content. Upon heating, the metastable tetragonal (cubic) phase is formed first. The higher the calcination temperature, the more likely is the formation of monoclinic zirconia. Crystalline zirconia appears at about 663 K in non-sulfated samples [212]. The crystallite size of the tetragonal phase and the fraction of the monoclinic phase increase with increasing calcination temperature [89, 212]. In the presence of sulfate, the tetragonal phase is stabilized, and even at temperatures of 933 K, purely tetragonal material can be obtained [212]. However, typically, formation of the monoclinic phase sets in at calcination temperatures above ca. 873 K [37]. The crystallite size of the metal oxide in sulfated zirconia, titania and tin oxide prepared via sulfate decomposition, was found to be constant up to the calcination temperature that provides the largest surface area [31].

The surface area of pure zirconia decreases with increasing calcination temperature above 773 K, with a smaller effect for materials with a small initial surface area [95, 101]. The surface area drops significantly once the temperature exceeds that of the glow exotherm [213]. Such a decrease is also observed for oxo-anion modified zirconia, for example for sulfated zirconia (from 135 $m^2\ g^{-1}$ at 773 K to 40 $m^2\ g^{-1}$ at 1173 K [53]), and for tungstated zirconia (from 100 $m^2\ g^{-1}$ at 973 K to 35 $m^2\ g^{-1}$ at 1223 K [99]). A linear correlation of surface area and temperature is seen between 773 and 1223 K [188]. The trends for different metal oxides are shown in Fig. 11. The sulfate content is also reduced by calcination, and this occurs in parallel with a loss of surface area, as Fig. 11 demonstrates. The published data vary as to the temperature where these losses start; values also depend on the initial sulfur content, and range from 473 K to 873 K [36, 37, 101, 212, 214]. It has been claimed that sulfate in certain crystallographic locations desorbs preferentially, and

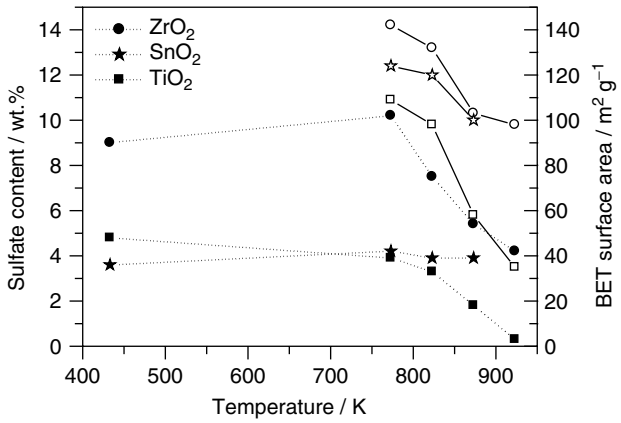

Fig. 11 Sulfate content (solid symbols) and BET surface area (open symbols) as a function of calcination temperature after drying at 433 K with oxide type as a parameter. (After Ref. [124].)

highly uncoordinated Zr^{4+} sites, which are strong Lewis acid sites, are generated at calcination above 773 K [215]. With increasing calcination temperature, the number of OH groups on the surface decreases [183].

2.3.9.7.4 **Effect of Calcination Temperature on Catalytic Performance** The best performance in *n*-butane isomerization is exhibited by sulfated zirconia that has been calcined at 823–873 K [187], 873 K [53], 893 K [216], or 875–900 K [214]. A minimum temperature of 773 K is required to obtain an active material [215]. Much higher temperatures are necessary for tungstated zirconia, about 1100–1200 K [99].

The initial activity of the obtained sulfated metal oxide catalyst in cumene cracking depends on the calcination temperature employed in decomposing the commercial $Zr(SO_4)_2$ or $Ti(SO_4)_2$ precursor. The activity increases with increasing calcination temperature, reaching a maximum at 900 K for the titania and 1000 K for the zirconia catalyst [114]. This increase in activity was found to be parallel to an increase in surface area [31].

The optimal temperature in the presence of promoters has been evaluated for sulfated zirconia promoted with Fe and Mn; the results are shown in Fig. 12 [217]. Because the activity of these catalysts changes rapidly, several data points representing different times on stream have been selected. The best performance is obtained after calcination at 923 K [166, 217].

2.3.9.7.5 **Effect of Holding Time** Little is known about the effect of holding time. Neither zirconia crystallization nor crystallite growth progress further after 2 h at $\geq$773 K [218]. If the temperature is high enough to decompose sulfate, e.g. 873 K, then the sulfate content will

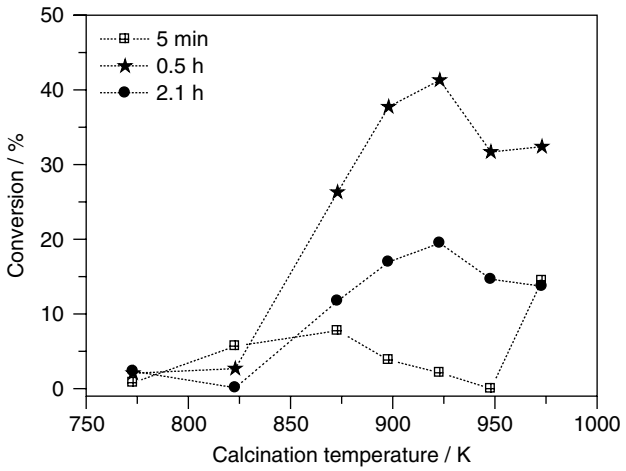

Fig. 12 Conversion at different times on stream for sulfated zirconia promoted with 1.5 wt.% Fe and 0.5 wt.% Mn. Calcination: 5 g raw material supported on frit in vertical open tube, 3 h heating phase to desired temperature, 4 h holding time, free air convection. Activation: 1.5 h at 723 K in N_2. Reaction conditions: 1.5 g catalyst, 0.5 kPa *n*-butane in N_2 at atmospheric pressure, 373 K, 80 mL min^{-1} total flow.

decrease with time [219]. Holding time and temperature have a combined effect, thus one can be selected if the other is adapted. For example, calcination for 12 h at 823 K delivers a promoted sulfated zirconia catalyst that yields equal conversion in alkane isomerization as one calcined for 4 h at 848 K [13].

2.3.9.7.6 **Calcination: A Summary** The calcination is a critical step, but it is difficult to name optimal conditions for two reasons.

First, phase composition, surface area, and oxo-anion content are interdependent properties. During calcination, excess sulfate or tungstate – that is, more than can be accommodated in a chemisorbed monolayer – will be converted to oxides, and more so as the surface area shrinks with increasing temperature. In the case of sulfate, oxide formation means volatilization and, in the case of tungstate, the excess remains in the sample in the form of WO_3 [99]. The sulfate content thus will be diminished; typical sulfur losses during calcination (2 h 873 K) depend on the sulfur loading and amount to 20–50% of the initial content [56]. Concurrent with sulfate loss and surface area shrinkage, monoclinization of zirconia may occur.

Second, the number of parameters influencing the outcome of calcination is high. Because of the condensation chemistry when starting from a hydrous oxide precursor, and the strongly exothermic crystallographic and morphological changes, both heat and mass transfer conditions are extremely important. The restriction of heat transfer and gas exchange seems favorable, contrary to IUPAC recommendations to use moving beds [58]. The most important point is to realize that simply stating the maximum temperature and holding time is insufficient; the bed size and packing, gas exchange conditions and heating rates must be specified and controlled to render calcinations reproducible.

2.3.9.8 **Sulfation of Thermally Treated Crystalline Oxides** It has often been claimed that adding sulfate to crystalline ZrO_2 does not yield an active catalyst [37], or yields only about one order of magnitude less active catalysts [214]. Specifically, the activity of the resultant materials drops when the hydrous oxide is pretreated at a temperature that will induce crystallization [2]. However, the situation is different for other oxides; for example, materials that are active in acid catalysis can be generated from Fe_2O_3 [220, 221].

2.3.9.8.1 **Sulfation with Aqueous Solutions (Solid–Liquid Phase)** The impregnation of zirconia, followed by calcination at 873 K, produces a material that is active in *n*-butane isomerization, with the activity related to the surface area [29]. Incipient wetness impregnation with ammonium sulfate and calcination at a temperature of at least 773 K also results in a sample active in *n*-butane isomerization [96].

2.3.9.8.2 **Sulfation via Gas Phase (Solid–Gas Phase)** SO_3 treatment at 573 K has been used to sulfate Fe_2O_3, with positive results in cyclopropane isomerization; also, H_2S and SO_2 treated Fe_2O_3 samples become active after oxidation at 723–773 K [221]. Equally, exposure of ZrO_2 to H_2S or SO_2, followed by treatment in an excess of O_2 at 723 K, yields virtually identical IR spectra [119]. Moreover, the spectra correspond to those obtained after aqueous solution impregnations using H_2SO_4, $(NH_4)_2SO_4$, or $Zr(SO_4)_2$ and suitable activation. At low coverage, monosulfate species are observed, while at more than 250 μmol S g^{-1} an S_2O_7-type species appears, indicating that a high sulfate density can be achieved via gas-phase reaction. It is possible to generate an active material via gas-phase sulfation of predominantly monoclinic zirconia using H_2SO_4 vapor [214].

SO_3 can also be employed as a sulfating agent. Exposure of zirconia supported on silica at 673 K generates a catalyst that is active in the transalkylation of benzene and diethylbenzene, though only after hydrating the material [222]. The sulfur content of sulfated zirconia can be increased by treatment with SO_3 at 673 K, with an increase from 0.44 to 0.64 mmol g^{-1} or 6 wt.% having

References see page 275

been reported [24]. In a series of samples, the total amount of sulfate after SO_3 treatment was found to be proportional to the fraction of monoclinic material in the sample, with loadings reaching 1.15 mmol g^{-1} or 12 wt.%. SO_3 treatment enhances the butane isomerization activity of sulfated zirconia, and zirconia becomes active. A sample prepared via SO_3 sulfation, and containing only 30% tetragonal zirconia, was even found to be catalytically more active than a sample created by the calcination of amorphous hydrous zirconia. Previous investigations have confirmed that monoclinic zirconia may be sulfated to give an active catalyst, but only at high sulfate loading and at the expense of low sulfate stability and rapid deactivation [223].

Calcination of pure hydrous zirconia leads to a lower surface area, and a monoclinic fraction is more easily formed. The successful sulfation of crystalline materials requires a high temperature; hence, it appears that a reaction of the sulfur species with the support must be initiated.

2.3.9.8.3 **Sulfation of Zirconia using Solid Sulfate Precursors** Kneading calcined zirconia (773 K) with ammonium sulfate, followed by a second calcination at 773 K, produces a material that is active for butene double-bond isomerization and the benzoylation of anisole [126].

2.3.9.9 Addition of Noble Metals

Noble metals can be added at different stages of the preparation, for example, during alkoxide hydrolysis [224], before calcination [225, 226], or after a calcination step [227]. Normal impregnation methods are employed; non-water-soluble noble metal salts can be kneaded together with the primary solid [225]. Noble metals are also effective when not located directly on the oxo-anion modified oxide [187].

2.3.9.10 Activation

Reports on the optimal activation temperature vary significantly. For sulfated zirconia, temperatures of 523–573 K [216], 573 K [228], 590 K [229], 673 K [94, 228], 723 K [55], or 923 K [214] have been reported as being optimal for high *n*-butane isomerization activity. The individual materials may favor different activation temperatures, but atmosphere, heating rates and holding times may also play a role.

The performance of promoted sulfated zirconia catalysts, for example with Fe and Mn as promoters, appears to be less sensitive to the temperature, particularly if the sample is activated in air and not in inert gas [152]. Temperatures of 623–723 K have been reported to generate the highest maximum activities [152, 166].

Noble metal-containing sulfated zirconia catalysts require a reduction step, with the inherent danger of reducing and volatilizing the sulfate. In the presence of Pt, the sulfate reduction temperature is shifted by about −200 K into the range 733 to 773 K [230]. The butane isomerization activity of Pt-doped sulfated zirconia decreases to zero with increasing reduction temperature in the range 583 to 693 K [46]. The situation will be more complicated if promoters are present; for example, Mn-promoted sulfated zirconia becomes inactive after treatment in 50% H_2 at 703 K [231].

Similar to sulfate, tungstate is much more easily reduced in the presence of Pt; W^{5+} species are formed at room temperature, but the systems are active [232]. Pt in Pt-doped Fe-promoted tungstated zirconia is reduced to metal at room temperature and hence, under hydroisomerization conditions, is also expected to be metallic, rendering an extra reduction step unnecessary [16].

2.3.9.11 Summary

The catalysts discussed in this chapter contain four types of components, namely matrix oxide, oxo-anion, promoter, and noble metal. If the oxide and oxo-anion precursors are associated in solution, then the metal cation's tendency for hydrolysis and for complexation with the oxo-anion will determine the nature of the primary solid. Alternatively, oxo-anions can be introduced to a solid hydrous or crystalline oxide.

If promoters are added, then the solid-state chemistry of the matrix oxide and its ability to accommodate foreign cations in its lattice come into play; on the other hand, oxo-ions will compete to form stable compounds with the promoter ions, e.g., $Al_2(SO_4)_3$. In the first case, the geometric and electronic structures of the matrix oxide can be tuned, although not independently. Thus, zirconia is an interesting matrix oxide for oxo-anion modification because, by varying its properties via promoter incorporation, the reactivity, e.g. the reducibility, of the oxo-anion can be determined.

All preparations require a high-temperature thermal treatment after associating the components. The calcination conditions are difficult to control because the reactions occurring in the sample consume and produce significant amounts of heat and gases; thus, heat- and mass-transfer conditions must be carefully considered. The thermal treatment represents a key step in the formation of oxo-anion modified oxide catalysts. As a consequence of the close interaction of the individual catalyst components, properties such as phase composition, surface area and oxo-anion content are interdependent, and determine further properties, such as acid site distribution. Therefore, the targeted synthesis of oxo-anion modified oxides with specific properties is challenging.

References

1. V. C. F. Holm, G. C. Bailey, US Patent 3, 032, 599, assigned to Phillips Petroleum Co., 1962.
2. M. Hino, S. Kobayashi, K. Arata, *J. Am. Chem. Soc.* **1979**, *101*, 6439.
3. M. Hino, K. Arata, *J. Chem. Soc., Chem. Commun.* **1980**, 851.
4. F. Schmidt, *Appl. Catal. A: General* **2001**, *221*, 15, and references therein.
5. N. Lohitharn, J. G. Goodwin, Jr., *J. Catal.* **2007**, *245*, 198.
6. G. D. Yadav, J. J. Nair, *Micropor. Mesopor. Mater.* **1999**, *33*, 1, and references therein.
7. X. Song, Y. Sayari, *Catal. Rev. -Sci. Eng.* **1996**, *38*, 329, and references therein.
8. K. Arata, M. Hino, *Mater. Chem. Phys.* **1990**, *26*, 213, and references therein.
9. C. D. Chang, F. T. DiGuiseppi, J. G. Santiesteban, US Patent 5, 780, 382, assigned to Mobil Oil Corporation, 1998.
10. K. Arata, *Appl. Catal. A: General* **1996**, *146*, 3, and references therein.
11. C. D. Chang, S. Han, R. A. Morrison, J. G. Santiesteban, US Patent 5, 999, 643, assigned to Mobil Oil Corporation, 1999.
12. P. T. Patil, K. M. Malshe, P. Kumar, M. K. Dongare, E. Kemnitz, *Catal. Commun.* **2002**, *3*, 411.
13. E. J. Hollstein, J. T. Wei, C. Y. Hsu, US Patent 4, 918, 041, assigned to Sun Refining and Marketing Co., 1990.
14. C.-Y. Hsu, C. R. Heimbuch, C. T. Armes, B. C. Gates, *J. Chem. Soc., Chem. Commun.* **1992**, 1645.
15. F. C. Lange, T.-K. Cheung, B. C. Gates, *Catal. Lett.* **1996**, *41*, 95.
16. S. Kuba, B. C. Gates, R. K. Grasselli, H. Knözinger, *Chem. Commun.* **2001**, 321.
17. R. Ahmad, J. Melsheimer, F. C. Jentoft, R. Schlögl, *J. Catal.* **2003**, *218*, 365.
18. S. Kuba, P. Lukinskas, R. Ahmad, F. C. Jentoft, R. K. Grasselli, B. C. Gates, H. Knözinger, *J. Catal.* **2003**, *219*, 376.
19. H. Liu, G. D. Lei, V. Adeeva, W. M. H. Sachtler, *J. Mol. Catal.* **1995**, *100*, 35.
20. S. Kuba, P. Lukinskas, R. K. Grasselli, B. C. Gates, H. Knözinger, *J. Catal.* **2003**, *216*, 353.
21. J. Luo, R. Stevens, *J. Am. Ceram. Soc.* **1999**, *82*, 1922.
22. C. Morterra, G. Cerrato, F. Pinna, M. Signoretto, *J. Catal.* **1995**, *157*, 109.
23. W. Stichert, F. Schüth, S. Kuba, H. Knözinger, *J. Catal.* **2001**, *198*, 277.
24. J. A. Moreno, G. Poncelet, *J. Catal.* **2001**, *203*, 453.
25. X. Li, K. Nagaoka, R. Olindo, J. A. Lercher, *J. Catal.* **2006**, *238*, 39.
26. X. Li, K. Nagaoka, L. J. Simon, J. A. Lercher, S. Wrabetz, F. C. Jentoft, C. Breitkopf, S. Matysik, H. Papp, *J. Catal.* **2005**, *230*, 214.
27. M. A. Risch, E. E. Wolf, *Appl. Catal. A: General* **1998**, *172*, L1.
28. C. Breitkopf, A. Garsuch, H. Papp, *Appl. Catal. A: General* **2005**, *296*, 148.
29. T. Riemer, D. Spielbauer, M. Hunger, G. A. H. Mekhemer, H. Knözinger, *J. Chem. Soc., Chem. Commun.* **1994**, 1181.
30. M. G. Cutrufello, U. Diebold, R. D. Gonzalez, *Catal. Lett.* **2005**, *101*, 5.
31. D. Fraenkel, *Ind. Eng. Chem. Res.* **1997**, *36*, 52.
32. S. Melada, M. Signoretto, F. Somma, F. Pinna, G. Cerrato, G. Meligrana, C. Morterra, *Catal. Lett.* **2004**, *94*, 193.
33. M. K. Mishra, B. Tyagi, R. V. Jasra, *Ind. Eng. Chem. Res.* **2003**, *42*, 5727.
34. D. Fărcaşiu, J. Q. Li, S. Cameron, *Appl. Catal. A: General* **1997**, *154*, 173.
35. J. C. Yori, J. M. Parera, *Appl. Catal. A: General* **1995**, *129*, L151.
36. P. Nascimento, C. Akratapoulou, M. Oszagyan, G. Coudurier, C. Travers, J. F. Joly, J. C. Vedrine, *Proceedings 10th International Congress on Catalysis*, July 19–24, 1992, Budapest, Hungary, *New Frontiers in Catalysis*, L. Guczi, F. Solymosi, P. Tetényi (Eds.), Elsevier, Amsterdam, 1993, p. 1185.
37. F. R. Chen, G. Coudurier, J.-F. Joly, J. C. Védrine, *J. Catal.* **1993**, *143*, 616.
38. A. Hofmann, J. Sauer, *J. Phys. Chem. B*, **2004**, *108*, 14652.
39. B. S. Klose, F. C. Jentoft, R. Schlögl. *J. Catal.* **2005**, *233*, 68.
40. B. S. Klose, Dissertation, Technische Universität Berlin, 2005, http://opus.kobv.de/tuberlin/volltexte/2005/1177/.
41. X. Li, K. Nagaoka, L. J. Simon, R. Olindo, J. A. Lercher, A. Hofmann, J. Sauer, *J. Am. Chem. Soc.* **2005**, *127*, 16159.
42. C. Breitkopf, H. Papp, X. Li, R. Olindo, J. A. Lercher, R. Lloyd, S. Wrabetz, F. C. Jentoft, K. Meinel, S. Förster, K.-M. Schindler, H. Neddermeyer, W. Widdra, A. Hofmann, J. Sauer, *Phys. Chem. Chem. Phys.* **2007**, *9*, 3600.
43. F. Babou, G. Coudurier, J. C. Védrine, *J. Catal.* **1995**, *152*, 341.
44. K. Biró, F. Figueras, S. Békássy, *Appl. Catal. A: General* **2002**, *229*, 235.
45. J. R. Sohn, S. H. Lee, *Appl. Catal. A: General* **2004**, *266*, 89.
46. K. Ebitani, J. Konishi, H. Hattori, *J. Catal.* **1991**, *130*, 257.
47. F.-S. Xiao, *Top. Catal.* **2005**, *35*, 9, and references therein.
48. V. M. Benítez, C. R. Vera, C. L. Pieck, F. G. Lacamoire, J. C. Yori, J. M. Grau, J. M. Parera, *Catal. Today* **2005**, *107–108*, 651.
49. R. Akkari, A. Ghorbel, N. Essayem, F. Figueras, *J. Sol-Gel Sci. Tech.* **2005**, *33*, 121.
50. R. Akkari, A. Ghorbel, N. Essayem, F. Figueras, *J. Sol-Gel Sci. Tech.* **2006**, *38*, 185.
51. X. Yang, R. E. Jentoft, F. C. Jentoft, *Catal. Lett.* **2006**, *106*, 195.
52. M. A. Ecormier, K. Wilson, A. F. Lee, *J. Catal.* **2003**, *215*, 57.
53. D. A. Ward, E. I. Ko, *J. Catal.* **1994**, *150*, 18.
54. B.-Y. Zhao, X.-P. Xu, H.-R. Ma, D.-H. Sun, J.-M. Gao, *Catal. Lett.* **1997**, *45*, 237.
55. H. K. Mishra, K. M. Parida, *Appl. Catal. A: General* **2002**, *224*, 179.
56. A. F. Bedilo, K. J. Klabunde, *J. Catal.* **1998**, *176*, 448.
57. D. J. Zalewski, S. Alerasool, P. K. Doolin, *Catal. Today* **1999**, *53*, 419.
58. J. Haber, J. H. Block, B. Delmon, *Pure Appl. Chem.* **1995**, *67*, 1257.
59. A. L. Hock, *Chemistry & Industry* **1974**, *2*, 864.
60. C. E. Morris, T. L. Vigo, C. M. Welch, *Textile Res. J.* **1981**, 90.
61. W. B. Blumenthal, *Ind. Eng. Chem.* **1954**, *46*, 528.
62. A. Clearfield, P. A. Vaughan, *Acta Crystallogr.* **1956**, *9*, 555.
63. G. M. Muha, P. A. Vaughan, *J. Chem. Phys.* **1960**, *33*, 194.
64. S. Hannane, F. Bertin, J. Bouix, *Bull. Soc. Chim. Fr.* **1990**, *127*, 43.
65. L. M. Toth, J. S. Lin, L. K. Felker, *J. Phys. Chem.* **1991**, *95*, 3106.
66. M. Åberg, J. Glaser, *Inorg. Chim. Acta* **1993**, *206*, 53.
67. K. Matsui, H. Suzuki, M. Ohgai, *J. Am. Ceram. Soc.* **1995**, *78*, 146.
68. A. Singhal, L. M. Toth, J. S. Lin, K. Affholter, *J. Am. Chem. Soc.* **1996**, *118*, 11529.

69. A. Singhal, L. M. Toth, G. Beaucage, J.-S. Lin, J. Peterson, *J. Colloid Interface Sci.* **1997**, *194*, 470.
70. K. Matsui, M. Ohgai, *J. Am. Ceram. Soc.* **1997**, *80*, 1949.
71. M. Z.-C. Hu, J. T. Zielke, J.-S. Lin, C. H. Byers, *J. Mater. Res.* **1999**, *14*, 103.
72. K. Lee, A. Sathyagal, P. W. Carr, A. V. McCormick, *J. Am. Ceram. Soc.* **1999**, *82*, 338.
73. P. Riello, A. Minesso, A. Craievich, A. Benedetti, *J. Phys. Chem. B.* **2003**, *107*, 3390.
74. R. E. Connick, W. H. McVey, *J. Am. Chem. Soc.* **1949**, *71*, 3182.
75. S. Ahrland, D. Karipides, B. Norén, *Acta Chem. Scand.* **1963**, *17*, 411.
76. A. Clearfield, *Rev. Pure Appl. Chem.* **1964**, *14*, 91.
77. E. Matijevic, *Acc. Chem. Res.* **1981**, *14*, 22.
78. R. Ruer, *Z. Anorg. Chem.* **1904**, *42*, 87.
79. F. G. Baglin, D. Breger, *Inorg. Nucl. Chem. Lett.* **1976**, *12*, 173.
80. U. Ciesla, M. Fröba, G. Stucky, F. Schüth, *Chem. Mater.* **1999**, *11*, 227.
81. M. Falinski, *Ann. Chim.* **1941**, *16*, 237.
82. M. Chatterjee, J. Ray, A. Chatterjee, D. Ganguli, *J. Mater. Sci. Lett.* **1989**, *8*, 548.
83. J. D'Ans, H. Eick, *Z. Elektrochem.* **1951**, *55*, 19.
84. I. J. Bear, W. G. Mumme, *Rev. Pure Appl. Chem.* **1971**, *21*, 189.
85. P. J. Squattrito, P. R. Rudolf, A. Clearfield, *Inorg. Chem.* **1987**, *26*, 4240.
86. O. Hauser, *Z. Anorg. Allg. Chem.* **1905**, *45*, 185.
87. I. G. Atanov, L. M. Zaitsev, *Russ. J. Inorg. Chem.* **1967**, *12*, 188.
88. H. Cölfen, H. Schnablegger, A. Fischer, F. C. Jentoft, G. Weinberg, R. Schlögl, *Langmuir* **2002**, *18*, 3500.
89. G. K. Chuah, S. Jaenicke, S. A. Cheong, K. S. Chan, *Appl. Catal. A: General* **1996**, *145*, 267.
90. R. Sui, A. S. Rizkalla, P. A. Charpentier, *Langmuir* **2006**, *22*, 4390.
91. G. K. Chuah, S. Jaenicke, B. K. Pong, *J. Catal.* **1998**, *175*, 80.
92. G. K. Chuah, S. Jaenicke, T. H. Xu, *Surf. Interface Anal.* **1999**, *28*, 131.
93. E. Riedel, *Anorganische Chemie*, 5th Ed., Walter deGruyter, Berlin, 2002, p. 776.
94. B. Li, R. D. Gonzalez, *Ind. Eng. Chem. Res.* **1996**, *35*, 3141.
95. G. K. Chuah, S. H. Liu, S. Jaenicke, J. Li, *Micropor. Mesopor. Mater.* **2000**, *39*, 381.
96. D. A. Ward, E. I. Ko, *J. Catal.* **1995**, *157*, 321.
97. D. Tichit, B. Coq, H. Armendariz, F. Figuéras, *Catal. Lett.* **1996**, *38*, 109.
98. V. Pârvulescu, S. Coman, P. Grange, V. I. Pârvulescu, *Appl. Catal. A: General* **1999**, *176*, 27.
99. R. A. Boyse, E. I. Ko, *J. Catal.* **1997**, *171*, 191.
100. H. Althues, S. Kaskel, *Langmuir* **2002**, *18*, 7428.
101. S. Melada, S. A. Ardizzone, C. L. Bianchi, *Micropor. Mesopor. Mater.* **2004**, *73*, 203.
102. S. Melada, M. Signoretto, S. A. Ardizzone, C. L. Bianchi, *Catal. Lett.* **2001**, *75*, 199.
103. C. T. Kresge, M. E. Leonowicz, W. J. Roth, J. C. Vartuli, *Nature* **1992**, *359*, 710.
104. F. Schüth, *Chem. Mater.* **2001**, *13*, 3184.
105. U. Ciesla, S. Schacht, G. D. Stucky, K. K. Unger, F. Schüth, *Angew. Chem.* **1996**, *108*, 597; U. Ciesla, S. Schacht, G. D. Stucky, K. K. Unger, F. Schüth, *Angew. Chem. Int. Ed. Eng.* **1996**, *35*, 541.
106. V. N. Romannikov, V. B. Fenelonov, E. A. Paukshtis, A. Yu. Derevyankin, V. I. Zaikovskii, *Micropor. Mesopor. Mater.* **1998**, *21*, 411.
107. D. M. Antonelli, *Adv. Mater.* **1999**, *11*, 487.
108. X. Yang, F. C. Jentoft, R. E. Jentoft, F. Girgsdies, T. Ressler, *Catal. Lett.* **2002**, *81*, 25.
109. Y. Sun, L. Yuan, W. Wang, C.-L. Chen, F.-S. Xiao, *Catal. Lett.* **2003**, *87*, 57.
110. www.zrchem.com, www.sigma-aldrich.com.
111. G. Hausinger, A. Reimer, J. Schönlinner, F. Schmidt, German patent application 100 33 477, Süd-Chemie AG, 2002.
112. R. D. Gillespie, M. Cohn, US Patent 6,706,659, assigned to UOP LLC, 2004.
113. F. C. Jentoft, A. Hahn, J. Kröhnert, G. Lorenz, R. E. Jentoft, T. Ressler, U. Wild, R. Schlögl, C. Häßner, K. Köhler, *J. Catal.* **2004**, *224*, 124, and references therein.
114. K. Arata, M. Hino, N. Yamagata, *Bull. Chem. Soc. Jpn.* **1990**, *63*, 244.
115. E. Escalona Platero, M. Peñarroya Mentruit, C. Otero Areán, A. Zecchina, *J. Catal.* **1996**, *162*, 268.
116. G. D. Yadav, A. D. Murkute, *J. Catal.* **2004**, *224*, 218.
117. Y. Xia, W. Hua, Z. Gao, *Appl. Catal. A: General* **1999**, *185*, 293.
118. R. L. Marcus, R. D. Gonzalez, E. L. Kugler, A. Auroux, *Chem. Eng. Commun.* **2003**, *190*, 1601.
119. M. Bensitel, O. Saur, J.-C. Lavalley, B. A. Morrow, *Mater. Chem. Phys.* **1988**, *19*, 147.
120. J. M. Parera, *Catal. Today* **1992**, *15*, 481.
121. D. Fărcaşiu, J. Q. Li, *Appl. Catal.* **1995**, *128*, 97.
122. C. D. Chang, F. T. DiGuiseppi, J. G. Santiesteban, US Patent 5, 780, 382, assigned to Mobil Oil Corporation, 1998.
123. J. B. Laizet, A. K. Søiland, J. Leglise, J. C. Duchet, *Top. Catal.* **2000**, *10*, 89.
124. A. Corma, A. Martínez, C. Martínez, *Appl. Catal. A: General* **1996**, *144*, 249.
125. D. F. Stec, R. S. Maxwell, H. Cho, *J. Catal.* **1998**, *176*, 14.
126. V. Quaschning, J. Deutsch, P. Druska, H.-J. Niclas, E. Kemnitz, *J. Catal.* **1998**, *177*, 164.
127. C. Miao, W. Hua, J. Chen, Z. Gao, *Catal. Lett.* **1996**, *37*, 187.
128. Z. Gao, Y. Xia, W. Hua, C. Miao, *Top. Catal.* **1998**, *6*, 101.
129. Y. D. Xia, W. M. Hua, Y. Tang, Z. Gao, *Chem. Commun.* **1999**, 1899.
130. W. Hua, Y. Xia, Y. Yue, Z. Gao, *J. Catal.* **2000**, *196*, 104.
131. P. Canton, R. Olindo, F. Pinna, G. Strukul, P. Riello, M. Meneghetti, G. Cerrato, C. Morterra, A. Benedetti, *Chem. Mater.* **2001**, *13*, 1634.
132. M. Perez-Luna, J. A. Toledo-Antonio, F. Hernandez-Beltrán, H. Armendariz, A. Garcia Borquez, *Catal. Lett.* **2002**, *83*, 201.
133. M. Hino, K. Arata, *React. Kin. Catal. Lett.* **2004**, *81*, 321.
134. M. Signoretto, S. Melada, F. Pinna, S. Polizzi, G. Cerrato, C. Morterra, *Micropor. Mesopor. Mater.* **2005**, *81*, 19.
135. J. C. Yori, J. M. Parera, *Appl. Catal. A: General* **1996**, *147*, 145.
136. R. Srinivasan, R. A. Keogh, B. H. Davis, *Appl. Catal. A: General* **1995**, *130*, 135.
137. T. Yamamoto, T. Tanaka, S. Takenaka, S. Yoshida, T. Onari, Y. Takahashi, T. Kosaka, S. Hasegawa, M. Kudo, *J. Phys. Chem. B* **1999**, *103*, 2385.
138. R. E. Jentoft, A. Hahn, F. C. Jentoft, T. Ressler, *J. Synchrotron Rad.* **2001**, *8*, 563.
139. M. A. Coelho, D. E. Resasco, E. C. Sikabwe, R. L. White, *Catal. Lett.* **1995**, *32*, 253.
140. E. A. García, E. H. Rueda, A. J. Rouco, *Appl. Catal. A: General* **2001**, *210*, 363.
141. M. Hino, K. Arata, *Catal. Lett.* **1996**, *34*, 125.

142. J. M. M. Millet, M. Signoretto, P. Bonville, *Catal. Lett.* **2000**, *64*, 135.
143. J. C. Yori, J. M. Parera, *Appl. Catal. A: General* **1995**, *129*, 83.
144. M. Perez-Luna, J. A. Toledo Antonio, A. Montoya, R. Rosas-Salas, *Catal. Lett.* **2004**, *97*, 59.
145. A. Corma, J. M. Serra, A. Chica, *Catal. Today* **2003**, *81*, 495.
146. M. L. Occelli, D. A. Schiraldi, A. Auroux, R. A. Keogh, B. H. Davis, *Appl. Catal. A: General* **2001**, *209*, 165.
147. C. T. Kresge, C. D. Chang, J. G. Santiesteban, D. S. Shihabi, S. A. Stevenson, J. C. Vartuli, US Patent 5, 902, 767, assigned to Mobil Oil Corporation, 1999.
148. A. Jatia, C. Chang, J. D. MacLeod, T. Okubo, M. E. Davis, *Catal. Lett.* **1994**, *25*, 21.
149. V. Adeeva, G. D. Lei, W. M. H. Sachtler, *Appl. Catal. A: General* **1994**, *118*, L11.
150. A. S. Zarkalis, C.-Y. Hsu, B. C. Gates, *Catal. Lett.* **1994**, *29*, 235.
151. V. Adeeva, J. W. de Haan, J. Jänchen, G. D. Lei, V. Schünemann, L. J. M. van de Ven, W. M. H. Sachtler, R. A. van Santen, *J. Catal.* **1995**, *151*, 364.
152. E. C. Sikabwe, M. A. Coelho, D. E. Resasco, R. L. White, *Catal. Lett.* **1995**, *34*, 23.
153. J. E. Tábora, R. J. Davis, *J. Chem. Soc., Faraday Trans.* **1995**, *91*, 1825.
154. K. T. Wan, C. B. Khouw, M. E. Davis, *J. Catal.* **1996**, *158*, 311.
155. R. Srinivasan, R. A. Keogh, A. Ghenciu, D. Fărcaşiu, B. H. Davis, *J. Catal.* **1996**, *158*, 502.
156. M. A. Coelho, W. E. Alvarez, E. C. Sikabwe, R. L. White, D. E. Resasco, *Catal. Today* **1996**, *28*, 415.
157. A. S. Zarkalis, C.-Y. Hsu, B. C. Gates, *Catal. Lett.* **1996**, *37*, 1.
158. M. Benaïssa, J. G. Santiesteban, G. Diaz, M. José-Yacamán, *Surf. Sci.* **1996**, *364*, L591.
159. X. Song, K. R. Reddy, A. Sayari, *J. Catal.* **1996**, *161*, 206.
160. C. Morterra, G. Cerrato, S. Di Ciero, M. Signorotto, A. Minesso, F. Pinna, G. Strukul, *Catal. Lett.* **1997**, *49*, 25.
161. W. E. Alvarez, H. Liu, D. E. Resasco, *Appl. Catal. A: General* **1997**, *162*, 103.
162. A. Sayari, Y. Yang, X. Song, *J. Catal.* **1997**, *167*, 346.
163. V. Adeeva, H.-Y. Liu, B.-Q. Xu, W. M. H. Sachtler, *Top. Catal.* **1998**, *6*, 61.
164. S. Rezgui, A. Liang, T.-K. Cheung, B. C. Gates, *Catal. Lett.* **1998**, *53*, 1.
165. F. C. Jentoft, *Erdöl, Erdgas, Kohle* **1998**, *114*, 441.
166. S. X. Song, R. A. Kydd, *Catal. Lett.* **1998**, *51*, 95.
167. D. R. Milburn, R. A. Keogh, D. E. Sparks, B. H. Davis, *Appl. Surf. Sci.* **1998**, *126*, 11.
168. M. Scheithauer, E. Bosch, U. A. Schubert, H. Knözinger, T.-K. Cheung, F. C. Jentoft, B. C. Gates, B. Tesche, *J. Catal.* **1998**, *177*, 137.
169. T. Tanaka, T. Yamamoto, Y. Kohno, T. Yoshida, S. Yoshida, *Jpn. J. Appl. Phys.* **1999**, *38*, 30.
170. A. Sayari, Y. Yang, *J. Catal.* **1999**, *187*, 186.
171. R. E. Jentoft, B. C. Gates, *Catal. Lett.* **2001**, *72*, 129.
172. T.-K. Cheung, J. L. d'Itri, F. C. Lange, B. C. Gates, *Catal. Lett.* **1995**, *31*, 153.
173. T.-K. Cheung, F. C. Jentoft, J. L. d'Itri, B. C. Gates, *Chem. Eng. Sci.* **1997**, *52*, 4607.
174. T.-K. Cheung, B. C. Gates, *Top. Catal.* **1998**, *6*, 41, and references therein.
175. A. S. Chelappa, R. C. Miller, W. J. Thomson, *Appl. Catal. A: General* **2001**, *209*, 359.
176. A. H. P. Hahn, T. Ressler, U. Wild, R. E. Jentoft, F. C. Jentoft, in preparation.
177. P. Li, I. W. Chen, J. E. Penner-Hahn, *Phys. Rev. B* **1993**, *48*, 10063, 10074, 10082.
178. J. Stöcker, R. Collongues, *Compt. Rend.* **1957**, *245*, 695.
179. H. J. Stöcker, *Ann. Chim.* **1960**, *5*, 1459.
180. J. Stöcker, *Bull. Soc. Chim.* **1961**, 78.
181. M. Yashima, N. Ishizawa, M. Yoshimura, *J. Am. Ceram. Soc.* **1992**, *75*, 1541, 1550.
182. D. Das, H. K. Mishra, A. K. Dalai, K. M. Parida, *Catal. Lett.* **2004**, *93*, 185.
183. B. S. Klose, F. C. Jentoft, R. Schlögl, I. R. Subbotina, V. B. Kazansky, *Langmuir* **2005**, *21*, 10564.
184. X.-R. Chen, C.-L. Chen, N.-P. Xua, S. Han, C.-Y. Mou, *Catal. Lett.* **2003**, *85*, 177.
185. X. Li, K. Nagaoka, J. A. Lercher, *J. Catal.* **2004**, *227*, 130.
186. E. A. Garcia, M. A. Volpe, M. L. Ferreira, E. H. Rueda, *Lat. Am. Appl. Res.* **2005**, *35*, 281.
187. K. Arata, H. Matsuhashi, M. Hino, H. Nakamura, *Catal. Today* **2003**, *81*, 17.
188. C. J. Norman, P. A. Goulding, I. McAlpine, *Catal. Today* **1994**, *20*, 313.
189. R. Srinivasan, D. Taulbee, B. H. Davis, *Catal. Lett.* **1991**, *9*, 1.
190. S. Chokkaram, R. Srinivasan, D. R. Milburn, B. H. Davis, *J. Colloid Interface Sci.* **1994**, *165*, 160.
191. T. Tatsumi, H. Matsuhashi, K. Arata, *Bull. Chem. Soc. Jpn.* **1996**, *69*, 1191.
192. J. Livage, K. Doi, C. Mazières, *J. Am. Ceram. Soc.* **1968**, *51*, 349.
193. A. Keshavaraja, N. E. Jacob, A. V. Ramaswamy, *Thermochim. Acta* **1995**, *254*, 267.
194. B. Djuricic, S. Pickering, D. McGarry, P. Glaude, P. Tambuyser, K. Schuster, *Ceram. Int.* **1995**, *21*, 195.
195. M. Sorrentino, L. Steinbrecher, F. Hazel, *J. Colloid Interface Sci.* **1969**, *31*, 307.
196. R. Srinivasan, B. H. Davis, *J. Colloid Interface Sci.* **1993**, *156*, 400.
197. K. Haberko, A. Ciesla, A. Pron, *Ceram. Int.* **1975**, *1*, 111.
198. R. Srinivasan, M. B. Harris, S. F. Simpson, R. J. De Angelis, B. H. Davis, *J. Mater. Res.* **1988**, *3*, 787.
199. P. D. L. Mercera, J. G. van Ommen, E. B. M. Doesburg, A. J. Burggraaf, J. R. H. Ross, *Appl. Catal.* **1990**, *57*, 127.
200. I. Molodetsky, A. Navrotsky, M. J. Paskowitz, V. J. Leppert, S. H. Risbud, *J. Non-Cryst. Solids* **2000**, *262*, 106.
201. S. Xie, E. Iglesia, A. T. Bell, *Chem. Mater.* **2000**, *12*, 2442.
202. I. Molodetsky, A. Navrotsky, M. Lajavardi, A. Brune, *Z. Phys. Chem.* **1998**, *207*, 59.
203. Y. Murase, E. Kato, *J. Am. Ceram. Soc.* **1983**, *66*, 196.
204. A. Hahn, T. Ressler, R. E. Jentoft, F. C. Jentoft, *Chem. Commun.* **2001**, 537 and electronic support information.
205. A. H. P. Hahn, R. E. Jentoft, T. Ressler, G. Weinberg, R. Schlögl, F. C. Jentoft, *J. Catal.* **2005**, *236*, 324.
206. J. Berzelius, *J. Chem. Phys.* (Schweigger, Nürnberg) **1812**, *6*, 119.
207. J. Berzelius, *Ann. Phys.* (Gilbert, Leipzig) **1812**, *42*, 276.
208. J. Berzelius, *J. Chem. Phys.* (Schweigger, Nürnberg) **1818**, *12*, 51.
209. R. Ruer, *Z. Anorg. Allg. Chem.* **1905**, *43*, 282.
210. L. Wöhler, *Koll.-Zeitschr.* **1926**, *38*, 97.
211. R. A. Keogh, R. Srinivasan, B. H. Davis, *J. Catal.* **1995**, *151*, 292.
212. R. A. Comelli, C. R. Vera, J. M. Parera, *J. Catal.* **1995**, *151*, 96.
213. B. H. Davis, *Catal. Today* **1994**, *20*, 219.
214. C. R. Vera, J. M. Parera, *J. Catal.* **1997**, *165*, 254.

215. C. Morterra, G. Cerrato, M. Signoretto, *Catal. Lett.* **1996**, *41*, 101.
216. S. X. Song, R. A. Kydd, *J. Chem. Soc. Faraday Trans.* **1998**, *94*, 1333.
217. F. C. Jentoft, B. C. Gates, unpublished results.
218. A. V. Chadwick, G. Mountjoy, V. M. Nield, I. J. F. Poplett, M. E. Smith, J. H. Strange, M. G. Tucker, *Chem. Mater.* **2001**, *13*, 1219.
219. X. Li, K. Nagaoka, L. J. Simon, R. Olindo, J. A. Lercher, *Catal. Lett.* **2007**, *113*, 34.
220. M. Hino, K. Arata, *Chem. Lett.* **1979**, 477.
221. T. Yamaguchi, T. Jin, K. Tanabe, *J. Phys. Chem.* **1986**, *90*, 3148.
222. I. J. Dijs, J. W. Geus, L. W. Jenneskens, *J. Phys. Chem. B* **2003**, *107*, 13403.
223. C. Morterra, G. Cerrato, F. Pinna, M. Signoretto, *J. Catal.* **1995**, *157*, 109.
224. M. Signoretto. F. Pinna, G. Strukul, G. Cerrato, C. Morterra, *Catal. Lett.* **1996**, *36*, 129.
225. M. Hino, K. Arata, *Catal. Lett.* **1995**, *30*, 25.
226. G. Larsen, L. M. Petkovic, *Appl. Catal. A: General* **1996**, *148*, 155.
227. S. Vijay, E. E. Wolf, *Appl. Catal. A: General* **2004**, *264*, 117.
228. M. Risch, E. E. Wolf, *Appl. Catal. A: General* **2001**, *206*, 283.
229. S. Y. Kim, J. G. Goodwin, Jr., D. Galloway, *Catal. Today* **2000**, *63*, 21.
230. C. R. Vera, J. C. Yori, C. L. Pieck, S. Irusta, J. M. Parera, *Appl. Catal. A: General* **2003**, *240*, 161.
231. R. E. Jentoft, A. H. P. Hahn, F. C. Jentoft, T. Ressler, *Phys. Chem. Chem. Phys.* **2005**, *7*, 2830.
232. S. Kuba, P. Concepción Heydorn, R. K. Grasselli, B. C. Gates, M. Che, H. Knözinger, *Phys. Chem. Chem. Phys.* **2001**, *3*, 146.

2.3.10 Catalysis by Ion-Exchange Resins

*Bruce C. Gates**

2.3.10.1 Introduction

Ion-exchange resins, typified by sulfonated crosslinked polystyrene, have been used widely in industry for many decades to catalyze reactions that are also catalyzed by mineral acids. These solid polymeric catalysts may be thought of as anchored sulfonic acid ($-SO_3H$) groups and solid analogues of sulfuric acid (or, more precisely, of toluenesulfonic acid). They were the first synthetic analogues of soluble molecular species to be used on a large scale as catalysts, having been applied in industry more than 60 years ago for esterification. Ion-exchange resins were the forerunners of what is now a large class of ''anchored'' catalysts that are solid analogues of soluble molecular or ionic species.

* Corresponding author.

Sulfonic acid resins are finding increasing application as replacements for soluble mineral acid catalysts, primarily because they minimize the detrimental environmental effects of acidic waste streams. Ion-exchange resin catalysts also offer the processing advantages of ease of separation from products and minimization of corrosion. These advantages are offset by their cost (they are much more expensive, per acid group, than mineral acids such as H_2SO_4 and HCl) and their relative lack of stability (see below).

The term ''ion-exchange resin'' refers to an organic polymeric resin that exchanges ions with a liquid that contains ions. Anion-exchange resins exchange anions, and cation-exchange resins exchange cations. For example, a resin with anchored $-SO_3H$ groups, in water, undergoes dissociation of these groups, giving (hydrated) protons and anchored sulfonate anions; cations from a solution in contact with the resin replace some of the protons. Thus, an aqueous solution containing Ca^{2+} ions will become enriched in hydrogen ions and depleted in Ca^{2+} ions as a result of contacting with the sulfonic acid resin. Sulfonic acid resins are used on a large scale in the purification of hard water. When anions such as Cl^- are replaced by OH^- from an anion-exchange resin and cations such as Ca^{2+} are replaced by H^+, the net effect is replacement of calcium chloride with water (an example of water softening).

The ion-exchange resins that are most important as industrial catalysts are sulfonic acid resins, and these are the principal topic of this chapter, the goals of which are to provide a summary of the synthesis and structural properties of these catalysts, with a summary of the most important catalytic applications and descriptions of the performance. The coverage of this subject here is not extensive, and earlier reviews [1–4] have provided more depth. The syntheses of these catalysts are described here only in broad terms, as key details remain proprietary. The inferences about catalyst structures are based on physical characterization methods that are also glossed over here.

Information closely complementing the content of the present chapter is available elsewhere in this Handbook (Chapter 13.10), which describes the synthesis of methyl *tert*-butyl ether (MTBE) and related ethers, which are manufactured on a large scale with sulfonic acid resin catalysts, and also in Chapter 10.6, in which details are described of the catalytic distillation that is applied with such catalysts in the manufacture of these ethers.

2.3.10.2 Classes of Ion-Exchange Resin Catalysts: The Importance of Porosity

When they were first prepared, ion-exchange resins were gels such as crosslinked polystyrene, and materials